nature physics

ARTICLES

PUBLISHED ONLINE: 29 JANUARY 2012 | DOI: 10.1038/NPHYS2207

Giant superfluorescent bursts from a semiconductor magneto-plasma

G. Timothy Noe II[1], Ji-Hee Kim[1], Jinho Lee[2], Yongrui Wang[3], Aleksander K. Wójcik[3], Stephen A. McGill[4], David H. Reitze[2], Alexey A. Belyanin[3] and Junichiro Kono[1]*

Superradiance—the cooperative decay of excited dipoles—has recently been discussed in a diverse range of contexts in which coherent coupling of constituent particles governs their cooperative dynamics: cavity quantum electrodynamics, quantum phase transitions and plasmonics. Here we observe intense, delayed bursts of coherent radiation from a photo-excited semiconductor and interpret it as superfluorescence, where macroscopic coherence spontaneously appears from initially incoherent electron–hole pairs. The coherence then decays superradiantly, with a concomitant abrupt decrease in population from full inversion to zero. This is the first observation of superfluorescence in a dense semiconductor plasma, where decoherence is much faster than radiative decay, a situation never encountered in atomic cases. Nonetheless, a many-body cooperative state of phased electron–hole 'dipoles' does emerge at high magnetic fields and low temperatures, producing giant superfluorescent pulses. The solid-state realization of superfluorescence resulted in unprecedented controllability, promising tunable sources of coherent pulses.

Quantum particles—electrons, atoms, molecules, electron–hole pairs and excitons—sometimes cooperate to develop a macroscopically ordered state with extraordinary properties, including superconducting states and Bose–Einstein condensates. In 1954, Dicke predicted that, when a macroscopic number of two-level dipoles are placed in a small volume, coherent coupling between dipoles develops by means of photon exchange, which results in cooperative recombination, or superradiance[1]. The concept of superradiance has not only been extensively studied in the context of quantum optics[2] but also been used recently in a variety of systems/phenomena, including quantum phase transitions[3] and plasmonics[4,5]. Here, we present an extreme form of superradiance—superfluorescence[6]—in an entirely new setting where a macroscopically ordered state develops spontaneously: an optically created dense electron–hole plasma in a semiconductor in a high magnetic field. Although optically excited semiconductors have attracted continuing interest for many years through endless discoveries associated with high-density electron–hole pairs, excitons and polaritons[7–13], the phenomenon we report here has never been observed. Namely, we create an ultradense electron–hole plasma with an intense femtosecond laser pulse and, after a certain delay, an ultrashort burst of coherent radiation emerges, which has a much higher intensity than the spontaneous emission of the same number of electron–hole pairs.

In the observed process, a macroscopic polarization spontaneously develops from an initially incoherent ensemble of electron–hole pairs and abruptly decays, producing giant pulses of light. Unlike superfluorescence previously observed in atomic systems, all processes occur on picosecond timescales and in a fully controllable fashion as a function of excitation laser power, magnetic field and temperature, opening up new opportunities for systematic many-body studies and the development of novel sources for coherent electromagnetic radiation. We performed theoretical simulations, based on the relaxation and recombination dynamics of ultrahigh-density electron–hole pairs in a quantizing magnetic field, that successfully captured the salient features of the experimental observations.

What distinguishes superfluorescence from any other light emission process is the existence of a self-organization stage during which macroscopic coherence, or a giant dipole, builds up spontaneously. This self-phasing stage manifests itself physically as a delay between the excitation pulse and the superfluorescent emission pulse. It is purely quantum mechanical in nature, driven by quantum fluctuations, and is a prerequisite for the subsequent appearance of superfluorescent bursts (Fig. 1a,b). Such bursts have enormous intensities, $\propto N^2$ (or $\propto N^{3/2}$ in extended samples[14]), where N is the number of excited dipoles in the ensemble. As Dicke described in his original paper[1], this emission process can be described through the dynamics of a Bloch vector, initially pointing 'north' (all dipoles are in the excited state and there is no coherence) and ending up pointing 'south' (all dipoles are in the ground state and, again, there is no coherence), emitting all its energy as light. The situation is analogous to a classical pendulum at an unstable equilibrium point (Fig. 1c), for which the rate of change of its angle (θ) from the vertical axis is proportional to $\sin\theta$, initially getting faster with increasing θ, becoming fastest at 90°, then slowing down and eventually stopping at 180°. This is a totally dissipative process: the initial fully inverted system is now stable in the ground state after releasing the superfluorescent burst of duration much shorter than the decoherence time, which is another distinctive feature of superfluorescence.

Superfluorescence has been observed in atomic gases[15,16] and rarefied impurities in glasses and crystals[17–19], but no direct evidence has been reported for superfluorescence using carriers in semiconductors. Our earlier CW measurements[20,21] indicated the possible existence of superfluorescence in semiconductor quantum

[1]Departments of Electrical and Computer Engineering and Physics and Astronomy, Rice University, Houston, Texas 77005, USA, [2]Department of Physics, University of Florida, Gainesville, Florida 32611, USA, [3]Department of Physics and Astronomy, Texas A&M University, College Station, Texas 77843, USA, [4]National High Magnetic Field Laboratory, Florida State University, Tallahassee, Florida 32310, USA. *e-mail: kono@rice.edu.

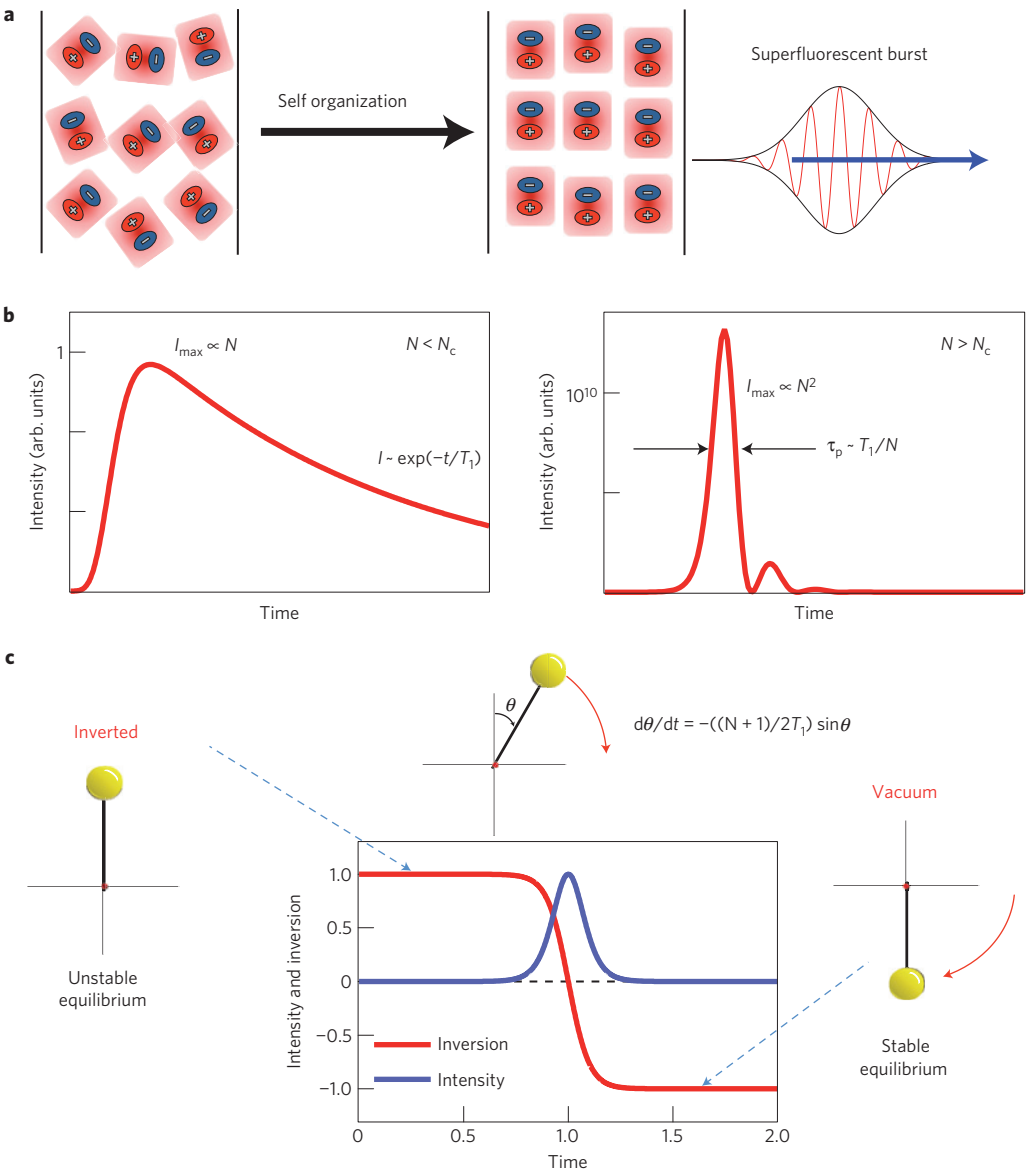

Figure 1 | Superfluorescence from a collection of dipoles (atoms, molecules, ions or excitons). a, Self-organization of dipoles and the resulting superfluorescent pulse. **b**, Characteristics of light emission dynamics after pulse excitation for weak (left) and strong (right) excitation. When the number of dipoles, N, is smaller than a critical value (N_c), the peak intensity is proportional to N and the intensity decays exponentially with a lifetime T_1. Under high excitation such that $N > N_c$, a delayed superfluorescent pulse appears with intensity proportional to N^2 and pulse width $\sim T_1/N$. **c**, Population inversion and emitted light intensity (normalized to the peak intensity) versus time (normalized to the pulse delay) for a superfluorescent system, together with Bloch vector dynamics analogous to the dynamics of an over-damped pendulum going from an unstable equilibrium position ($\theta = 0°$) to the stable ground state ($\theta = 180°$) by releasing all its energy as a burst of superfluorescence.

wells in high magnetic fields, but did not directly detect bursts of superfluorescence in the time domain. Note that superradiance studies previously reported for semiconductors[22,23] and polymers[24] are distinctly different from superfluorescence—they either deal with an accelerated decay of a single exciton due to translational symmetry breaking in a low-dimensional structure or refer to the cooperative enhancement of recombination rates in coherently prepared excitons that does not involve the above-described self-phasing process, an essential ingredient of superfluorescence[6,14,25]. An accelerated radiative decay of excitons was observed in ref. 26, which the authors interpreted as superfluorescence from a Bose–Einstein condensate of excitons bound to defects.

The sample used in this study was a stack of fifteen undoped quantum wells consisting of 8 nm $In_{0.2}Ga_{0.8}As$ wells and 15 nm GaAs barriers. The confinement of the well resulted in quantized energy subbands for electrons in the conduction band and holes in the valence band. The strain present in this sample resulted in a large splitting of the heavy-hole (H_1) and light-hole (L_1) states (Fig. 2a), with only the heavy-hole states being relevant to the present study. On optical excitation using a Ti:sapphire laser with photon energy centred at 1.55 eV, carriers are excited above the bandgap of the GaAs barriers. Both the electrons and holes then experience many scattering events before relaxing into the quantum well to form two-dimensional magneto-excitons. We employ the high-field Landau level notation, (NM), to specify each magneto-exciton state, where N (M) is the electron (hole) Landau level index. The three lowest-energy, dipole-allowed transitions that we primarily study in this work are the $(NM) = (00)$, (11) and (22) transitions, which correspond to the 1s, 2s and 3s transitions using the low-field excitonic notation[27].

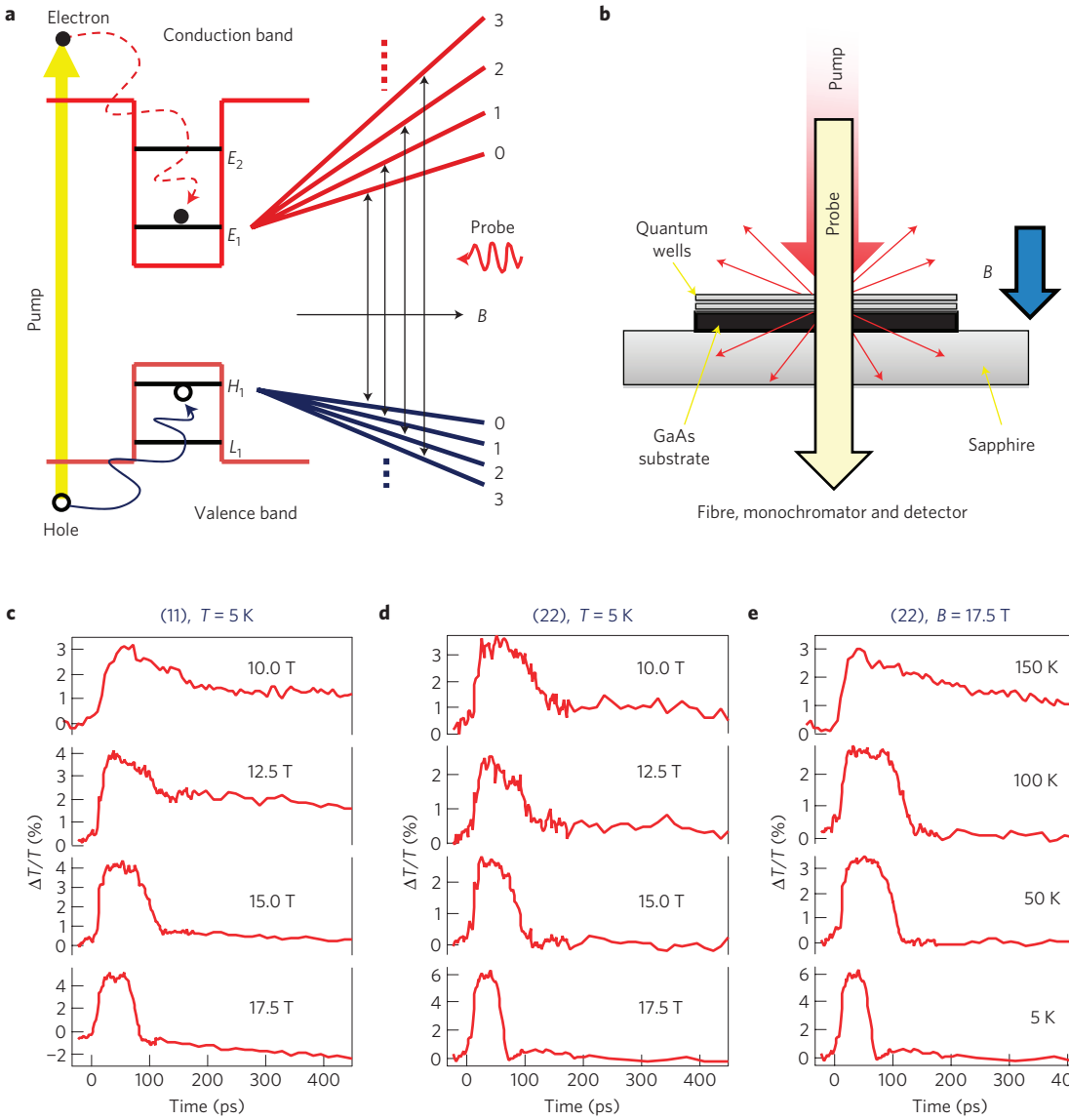

Figure 2 | Observation of a sudden population drop through ultrafast pump–probe spectroscopy. a, Sample studied and schematic diagram of energy levels in the system. **b**, Experimental configuration of pump–probe measurements. **c**, Pump–probe data for the (11) level at different magnetic fields at 5 K. **d**, Pump–probe data for the (22) level at different magnetic fields at 5 K. **e**, Pump–probe data for the (22) level at 17.5 T at different temperatures.

Pump–probe measurements were made in a transmission geometry in the Faraday configuration (Fig. 2b), where the pump and probe beams were parallel to the magnetic field and incident normal to the quantum wells. The differential transmission, $\Delta T/T$, when tuned to a particular transition, is proportional to the population inversion for that transition, which is equal to the difference between the number of occupied and unoccupied exciton states. Figure 2c,d demonstrates that at the lowest temperature, 5 K, there is a sudden decrease in population inversion when the magnetic field, B, is higher than 10 T. At lower B, the population dynamics of the (11) transition exhibits a typical long exponential decay, as seen in Fig. 2c. With increasing B, the exponential decay transforms into a sudden decrease that becomes faster and occurs at a shorter time delay, ~80 ps, for the (11) transition at 17.5 T. The (22) transition under the same conditions shows similar results, except that the sudden decrease in population occurs at an even shorter delay time, ~60 ps, for the highest B, as shown in Fig. 2d. Finally, Fig. 2e shows that decreasing the temperature, T, and increasing B have a similar effect, that is, the change in population becomes more sudden and occurs at a shorter time delay when T changes from 150 K to 5 K.

Spectrally and temporally resolved photoluminescence, collected in the geometry depicted in Fig. 3a, revealed superfluorescent pulses under various B, T and pump conditions, as shown in Fig. 3b–g. Figure 3b shows time-resolved photoluminescence data at 17.5 T and 5 K, spectrally selected for the (00) transition, taken with pump pulse energies, 0.25 nJ and 10 μJ, to be compared with Fig. 1b. For weak excitation (0.25 nJ), the photoluminescence, measured from the centre fibre, shows an initial slow increase due to exciton formation, followed by interband relaxation with an exponential decay time of hundreds of picoseconds. The photoluminescence measured from the edge fibre provided a similar decay, but the signal was ~40 times lower, indicating that the emission under weak excitation is typical spontaneous emission radiated in all directions with equal probability. In contrast, for strong excitation (10 μJ), we observe a giant, delayed pulse of radiation from the edge fibre. The photoluminescence measured in the centre fibre showed no pulse of radiation and the peak intensity was ~100 times lower. Quantitatively, Fig. 3b shows that an increase in pump pulse energy by roughly four orders of magnitude results in a

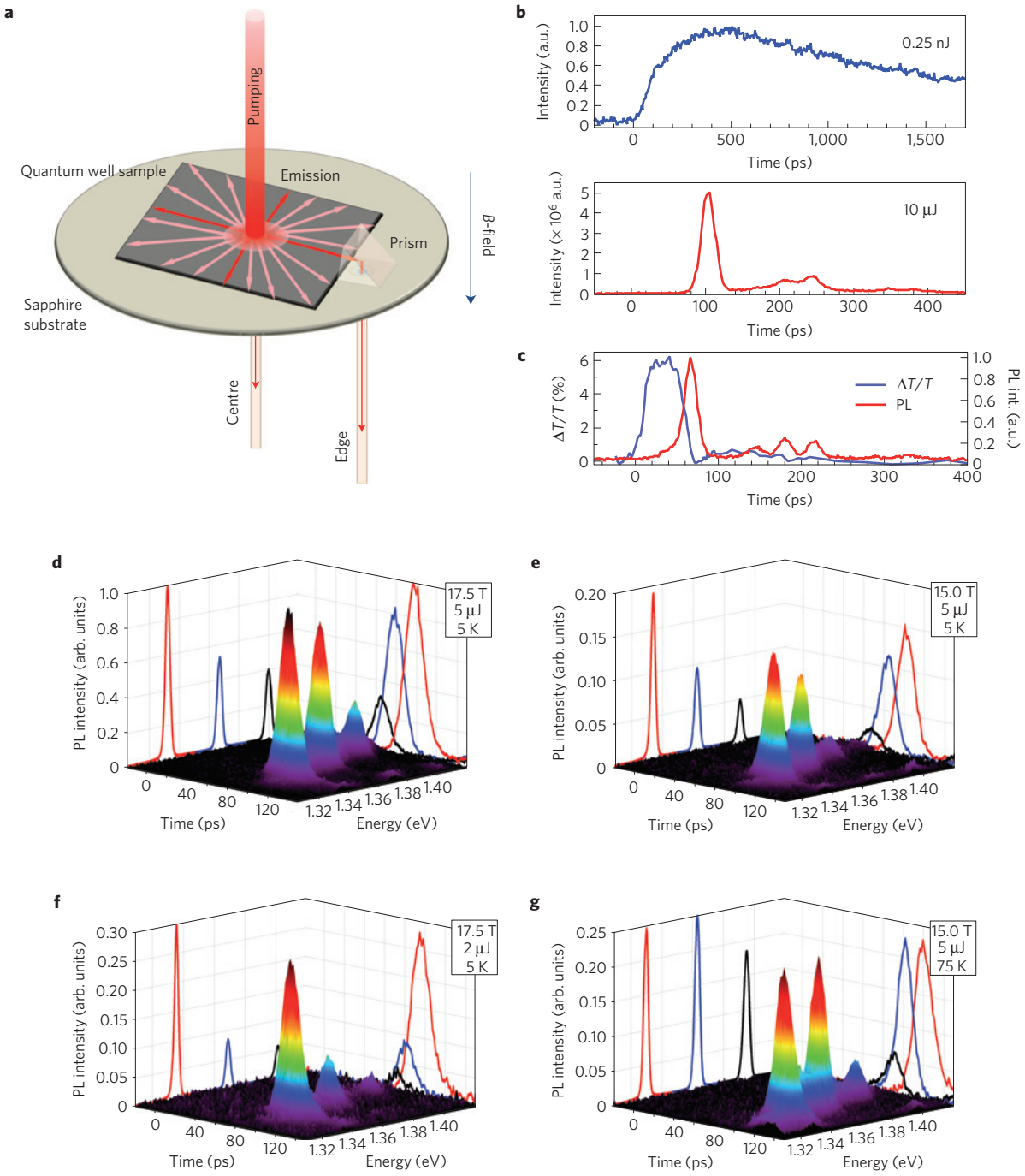

Figure 3 | Observation of delayed bursts of radiation through time-resolved photoluminescence spectroscopy. a, Set-up. **b**, Time-resolved emission for weak (top) and strong (bottom) excitation for the (00) transition at 17.5 T and 5 K. This should be compared with Fig. 1b. **c**, Comparison between pump–probe data and time-resolved photoluminescence (PL) for the (22) level at 17.5 T and 5 K, demonstrating the temporal coincidence between the population drop in pump–probe differential transmission and emission of the giant pulse of radiation. This should be compared with Fig. 1c. **d**–**g**, Streak camera images of emission intensity as a function of photon energy and delay time at 17.5 T, 5 μJ pump pulse energy and 5 K (**d**), 15.0 T, 5 μJ pump pulse energy and 5 K (**e**), 17.5 T, 2 μJ pump pulse energy and 5 K (**f**) and 17.5 T, 5 μJ pump pulse energy and 75 K (**g**). In **d**–**g**, the left hand panels show the time-integrated emission spectra, with the (00) peak in red, (11) in blue and (22) in black, while the right hand panels show time-resolved slices at the peak positions of the (00), (11) and (22) transitions.

peak emission intensity that is roughly six orders of magnitude larger. This is in agreement with the expected $N^{3/2}$-dependence for superfluorescence in extended samples[14], where N is the number of excited dipoles (electron–hole pairs in the present case). These results indicate that with increasing magnetic field strength, increasing pump pulse energy and decreasing temperature, the regime of light emission undergoes a transition from ordinary spontaneous emission to superfluorescence dominating the in-plane emission at high pump-pulse energy. Figure 3c overlays pump–probe and time-resolved photoluminescence data taken under the same conditions for the (22) transition, where we see that the appearance of the giant emission pulse coincides in time with the abrupt population drop from its maximum value to zero. This is in stark contrast with the dynamics of ordinary single-pass

amplifiers, where a pulse of the amplified spontaneous emission would consume at most half of the population.

Figure 3d shows a photoluminescence intensity map as a function of delay time and photon energy at 17.5 T, 5 K and 5 μJ. Pulses of superfluorescence coming from the (00), (11) and (22) transitions are clearly resolved, both in time and energy. For each transition, a large pulse of radiation appears after some delay time. The highest-energy transition, (22), emits a pulse first, and each lower-energy transition emits a pulse directly after the transition just above it. Figure 3e shows the effects of lowering B to 15 T: (1) the separation between Landau levels decreases (compare the left-hand panels of Fig. 3d,e), (2) the emission of superfluorescence occurs at later delay times for a given transition (compare the right-hand panels of Fig. 3d,e), and (3) the superfluorescent pulse intensity decreases (compare Fig. 3d,e). With decreasing pump pulse energy, we see the emission decrease dramatically (compare Fig. 3d,f). With increasing T, the emission from all transitions weakens significantly and moves to later delay times (Fig. 3g); the emission energies decrease with increasing T owing to bandgap shrinkage.

These pump–probe and time-resolved photoluminescence results are consistent with the expected conditions required to make superfluorescent emission possible. In particular, the B and T dependence of the population drop and superfluorescent emission intensity can be explained as follows. The key parameter determining the growth rate of superfluorescence is the cooperative frequency, ω_c, which must exceed the dephasing rate of the optical polarization associated with a given recombination transition for superfluorescence to be observable[14]. Specifically, to observe superfluorescence from electron–hole pairs in a semiconductor quantum well, the condition

$$\omega_c = \sqrt{\frac{8\pi^2 d^2 n \Gamma c}{\hbar \bar{n}^2 \lambda L_{QW}}} \geq \frac{2}{T_2}$$

must be satisfied[20,21], where d is the transition dipole moment, n is the 2D electron–hole density, Γ is the overlap factor of radiation with the quantum wells, $\hbar$ is the reduced Planck constant, $\bar{n}$ is the refractive index, λ is the wavelength, c is the speed of light, L_{QW} is the total width of the quantum wells and T_2 is the dephasing time of the optical polarization. A magnetic field increases d, n and T_2, making it easier to establish the macroscopic coherence required for superfluorescent emission. Quantitatively, d increases by a factor of three for the (22) transition when B increases from 0 T to 17 T, because of an increased overlap of electron and hole wave functions, and thus, the growth rate in the active region increases to 5–10 ps^{-1}. Increasing T decreases T_2, making it more difficult to establish the macroscopic coherence. A high B and low T strongly suppress all scattering processes in the lowest Landau levels because these states are almost completely occupied with carriers whereas empty states are located high above. Under these conditions one can expect T_2 to be on the scale of tens of picoseconds.

We simulated the dynamics of superfluorescence in quantum wells by calculating the eigenstates and eigenfunctions of the relevant states, deriving the matrix elements of the optical transitions and phonon scattering, and solving the coupled density-matrix and wave equations for exciton populations, interband coherences and optical fields (see Methods for details). Figure 4 shows the dynamics of electron–hole pair population and edge-propagating radiation intensity calculated for the (22) state at 17 T. Here, we assumed a T_2 of 50 ps (or a dephasing rate of 0.02 ps^{-1}), while the calculated modal growth rate of superfluorescence for this case was 0.3 ps^{-1}. As seen in Fig. 4, all states are fully occupied within the first few picoseconds, with their population n saturating, corresponding to the plateaux observed in the pump–probe measurements of Fig. 2. After a delay time

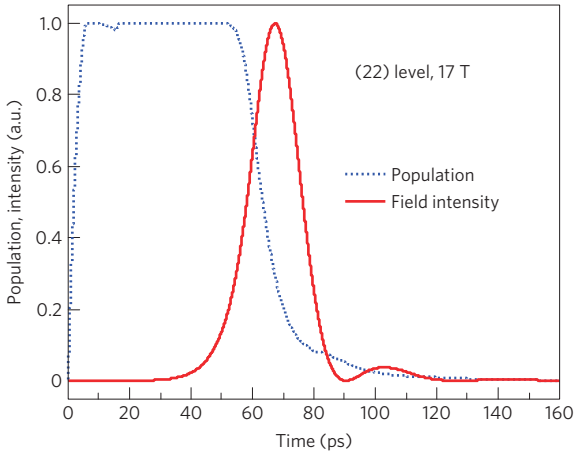

Figure 4 | Theoretical simulations of superfluorescence from an ultradense electron–hole plasma in a semiconductor quantum well in a perpendicular magnetic field of 17 T. Occupation number of excitons on the (22) level (blue dashed line) and normalized electromagnetic field intensity of superfluorescence from the (22) level (red solid line) as a function of time since the beginning of the pump pulse. A population equal to one corresponds to total inversion where all states are fully occupied by excitons.

of about 60 ps, a superfluorescent pulse emerges, with a duration of 10–20 ps (shorter than T_2). The emission consumes nearly all the population, bringing the effective population inversion of the (22) level $\Delta n = 2n - 1$ from +1 to −1. Note that a pulse of amplified spontaneous emission would consume only half of the population, bringing n to 1/2 and Δn to zero. Overall, there is excellent agreement between the simulations and the pump–probe and time-resolved photoluminescence data of Fig. 3. The dynamics of superfluorescence from (11) and (00) Landau levels is similar to that of the (22) level, except that the superfluorescent pulse from lower Landau levels develops at later times and has a higher intensity, again in agreement with the experiment.

It is important to point out that, whereas there is a certain analogy between recombination of electron–hole pairs (or excitons) and radiative transitions in atoms, there is no a priori reason for superfluorescence in semiconductors to be similar to atomic superfluorescence (or even to exist at all). In fact, all previous observations of superfluorescence were made in low-density atomic systems, where any decoherence processes were negligible and the only relevant decay was by means of radiative coupling. In the present case, however, we deal with an ultradense electron–hole plasma in a semiconductor, a complex many-body system with a variety of ultrafast interactions. The decoherence rates are at least 1,000 times faster than the rate of the radiative decay of individual excitons, a new regime totally unexplored in previous atomic superfluorescence studies. We have shown, nonetheless, that collective many-body coupling of electron–hole pairs by means of a common radiation field does develop under certain conditions and leads to the spontaneous formation of a macroscopic optical polarization from an initially completely incoherent state.

Finally, the solid-state realization of superfluorescence in the present work resulted in an unprecedented degree of controllability in the generation of superfluorescence, promising new opportunities for both fundamental many-body studies and device applications. We clearly demonstrated that the intensity, duration and delay time of superfluorescent bursts are tunable through B, T and pump laser power. Namely, unlike atoms, we can tune virtually everything: the density of states, the oscillator strength, the transition frequencies and, most importantly, the decoherence times using B and T. The fact that B affects both the

characteristics of superfluorescence and the strength of Coulomb interaction can lead to interesting aspects of superfluorescence in a way that other systems cannot. Furthermore, we can make use of advanced semiconductor technology and design compact superfluorescence-based devices, contingent on the degree to which the strong B and low T requirements can be lessened by sample design improvements. For example, by increasing the number of quantum wells or surrounding them with symmetric cladding layers, the electromagnetic superfluorescent modes can be guided in the active region, increasing the modal overlap and enhancing the superfluorescence growth rate to the order of 3–5 ps^{-1}. In this case, one should expect to observe much shorter pulses and delay times, and superfluorescence should survive at higher dephasing rates and become observable even at room temperature. Eventually, an electrically driven device for producing coherent superfluorescent pulses with any desired wavelength could be developed by using existing technologies of semiconductor quantum engineering.

Methods

Pump–probe and time-resolved photoluminescence measurements. We used an amplified Ti:sapphire laser as the pump and a tunable optical parametric amplifier to probe the population inversion of the (00), (11), and (22) transitions as a function of time using standard delay stage pump–probe techniques. The sample was placed in a 17.5 T superconducting magnet in the Faraday geometry, where the field was parallel to the optical excitation and perpendicular to the plane of the quantum well. The pump and probe beams were made collinear before entering the magnet bore through a CaF_2 window. The probe beam was collected by an optical fibre to bring the light out of the magnet, then filtered using a small monochromator before being detected with a silicon photodiode. The measurement used a lock-in amplifier set to the modulation frequency of an optical chopper introduced in the path of the pump line. We measured the time-resolved photoluminescence using a streak camera with 2 ps resolution. The sample was attached to a sapphire window, and a right-angle microprism was mounted at the edge of the sample to redirect the in-plane emission into an edge collection fibre (Fig. 3a). The output of the fibres was f-number matched with a spectrometer so that the photoluminescence could be spectrally separated before entering the streak camera.

Modelling. Theoretical modelling of superfluorescence starts by calculating the eigenstates and eigenfunctions for electron-heavy hole quantum-well magneto-excitons following the steps outlined in ref. 28. These eigenfunctions are used to derive matrix elements of the optical transitions and phonon scattering rates. Then we solve a coupled set of space- and time-dependent density-matrix and wave equations for exciton populations, interband coherences (off-diagonal density-matrix elements) and optical fields. As all the photo-created carriers eventually occupy the lowest Landau levels to near-complete degeneracy, before the superfluorescent pulses are formed, we include only the (00), (11) and (22) states. The initial kinetics of carrier cooling and relaxation are modelled by an effective scattering rate to the (22) state, which is assumed to be a pulse of amplitude 0.1–1 ps^{-1} with an exponential decay time of ~10 ps. The dominant interaction between excitons which leads to the formation of superfluorescent pulses is through their coupling to a common electromagnetic mode. Other interactions between excitons are ignored as they are not essential to the superfluorescence dynamics, although they do renormalize the transition energies and Rabi frequencies.

See Supplementary Information for full methods and associated references.

Received 19 September 2011; accepted 9 December 2011; published online 29 January 2012

References

1. Dicke, R. H. Coherence in spontaneous radiation processes. *Phys. Rev.* **93,** 99–110 (1954).
2. Scully, M. O. & Svidzinsky, A. A. The super of superradiance. *Science* **325,** 1510–1511 (2009).
3. Baumann, K., Guerlin, C., Brennecke, F. & Esslinger, T. Dicke quantum phase transition with a superfluid gas in an optical cavity. *Nature* **464,** 1301–1306 (2010).
4. Sonnefraud, Y. *et al.* Experimental realization of subradiant, superradiant, and Fano resonances in ring/disk plasmonic nanocavities. *ACS Nano* **4,** 1664–1670 (2010).
5. Martín-Cano, D., Martín-Moreno, L., García-Vidal, F. J. & Moreno, E. Resonance energy transfer and superradiance mediated by plasmonic nanowaveguides. *Nano Lett.* **10,** 3129–3134 (2010).
6. Bonifacio, R. & Lugiato, L. A. Cooperative radiation processes in two-level systems: Superfluorescence. *Phys. Rev. A* **11,** 1507–1521 (1975).
7. Chemla, D. S. & Shah, J. Many-body and correlation effects in semiconductors. *Nature* **411,** 549–557 (2001).
8. Butov, L. V., Lai, C. W., Ivanov, A. L., Gossard, A. C. & Chemla, D. S. Towards Bose–Einstein condensation of excitons in potential traps. *Nature* **417,** 47–52 (2002).
9. Kasprzak, J. *et al.* Bose–Einstein condensation of exciton polaritons. *Nature* **443,** 409–414 (2006).
10. Li, X., Zhang, T., Borca, C. N. & Cundiff, S. T. Many-body interactions in semiconductors probed by optical two-dimensional Fourier transform spectroscopy. *Phys. Rev. Lett.* **96,** 057406 (2006).
11. Balili, R., Hartwell, V., Snoke, D., Pfeiffer, L. & West, K. Bose–Einstein condensation of microcavity polaritons in a trap. *Science* **316,** 1007–1010 (2007).
12. Turner, D. B. & Nelson, K. A. Coherent measurements of high-order electronic correlations in quantum wells. *Nature* **466,** 1089–1092 (2010).
13. Deng, H., Haug, H. & Yamamoto, Y. Exciton-polariton Bose–Einstein condensation. *Rev. Mod. Phys.* **82,** 1489–1537 (2010).
14. Zheleznyakov, V. V., Kocharovskii, V. V. & Kocharovskii, Vl. V. Polarization waves and super-radiance in active media. *Sov. Phys. Usp.* **32,** 835–870 (1989).
15. Skribanowitz, N., Herman, I. P., MacGillivray, J. C. & Feld, M. S. Observation of Dicke superradiance in optically pumped HF gas. *Phys. Rev. Lett.* **30,** 309–312 (1973).
16. Gibbs, H. M., Vrehen, Q. H. F. & Hikspoors, H. M. J. Single-pulse superfluorescence in cesium. *Phys. Rev. Lett.* **39,** 547–550 (1977).
17. Florian, R., Schwan, L. O. & Schmid, D. Superradiance and high-gain mirrorless laser activity of O_2^--centers in KCl. *Solid State Commun.* **42,** 55–57 (1982).
18. Malcuit, M. S., Maki, J. J., Simkin, D. J. & Boyd, R. W. Transition from superfluorescence to amplified spontaneous emission. *Phys. Rev. Lett.* **59,** 1189–1192 (1987).
19. Zinov'ev, P. V. *et al.* Superradiance in a diphenyl crystal containing pyrene. *Sov. Phys. JETP* **58,** 1129–1133 (1983).
20. Jho, Y. D. *et al.* Cooperative recombination of a quantized high-density electron–hole plasma in semiconductor quantum wells. *Phys. Rev. Lett.* **96,** 237401 (2006).
21. Jho, Y. D. *et al.* Cooperative recombination of electron–hole pairs in semiconductor quantum wells under quantizing magnetic fields. *Phys. Rev. B* **81,** 155314 (2010).
22. Björk, G., Pau, S., Jacobson, J. & Yamamoto, Y. Wannier exciton superradiance in a quantum-well microcavity. *Phys. Rev. B* **50,** 17336–17348 (1994).
23. Ding, C. R. *et al.* Super-radiance of excitons in a single ZnO nanostructure. *Appl. Phys. Lett.* **93,** 151902 (2008).
24. Meinardi, F., Cerminara, M., Sassella, A., Bonifacio, R. & Tubino, R. Superradiance in molecular H aggregates. *Phys. Rev. Lett.* **91,** 247401 (2003).
25. Siegman, A. E. *Lasers* 547–557 (Univ. Science Books, 1986).
26. Dai, D. C. & Monkman, A. P. Observation of superfluorescence from a quantum ensemble of coherent excitons in a ZnTe crystal: Evidence for spontaneous Bose–Einstein condensation of excitons. *Phys. Rev. B* **84,** 115206 (2011).
27. Jho, Y. D *et al.* Role of Coulomb interactions in dark-bright magneto-exciton mixing in strained quantum wells. *Phys. Rev. B* **72,** 045340 (2005).
28. Lee, J. *et al.* Robust, stable single-exciton emission from an ultrahigh-density magneto-plasma. Preprint at http://arxiv.org/abs/1009.3067v1 (2010).

Acknowledgements

This work was supported by the National Science Foundation through grants DMR-1006663 and ECS-0547019. A portion of this work was performed at the National High Magnetic Field Laboratory, supported by NSF Co-operative Agreement No. DMR-0084173 and by the State of Florida. We thank G. Solomon for providing us with the InGaAs/GaAs quantum well sample used in this study.

Author contributions

G.T.N., J-H.K. and J.L. performed the measurements presented in this manuscript, in collaboration with S.A.M. J.L. did most of the initial work of setting up the streak camera. Y.W., A.K.W. and A.A.B. developed the theoretical model and performed simulations. D.H.R. and J.K. provided overall supervision and guidance on the experimental aspects. All authors contributed to data analysis and interpretation as well as the writing of the manuscript.

Additional information

The authors declare no competing financial interests. Supplementary information accompanies this paper on www.nature.com/naturephysics. Reprints and permissions information is available online at www.nature.com/reprints. Correspondence and requests for materials should be addressed to J.K.